

Turbulence Stress Measurements in a Nonadiabatic Hypersonic Boundary Layer

V. Mikulla* and C.C. Horstman†
Ames Research Center, NASA, Moffett Field, Calif.

Turbulent shear stress and direct turbulent total heat-flux measurements have been made across a nonadiabatic, zero pressure gradient, hypersonic boundary layer by using specially designed hot-wire probes free of strain-gauging and wire oscillation. Heat-flux measurements were in reasonably good agreement with values obtained by integrating the energy equation using measured profiles of velocity and temperature. The shear-stress values deduced from the measurements, by assuming zero correlation of velocity and pressure fluctuations, were lower than the values obtained by integrating the momentum equation. Statistical properties of the cross-correlations are similar to corresponding incompressible measurements at approximately the same momentum-thickness Reynolds number.

Nomenclature

C_p	= specific heat at constant pressure
e	= hot-wire voltage
f	= frequency
H	= stagnation enthalpy
M	= Mach number
p	= pressure
$R_{(\rho u)'v'}$	= correlation coefficient of mass flux and vertical velocity fluctuations, $[(\rho u)'v'] / [\langle (\rho u)' \rangle \langle v' \rangle]$
$R_{(\rho u)'w'}$	= correlation coefficient of mass flux and lateral velocity fluctuations, $[(\rho u)'w'] / [\langle (\rho u)' \rangle \langle w' \rangle]$
$R_{(\rho u)'T_t'}$	= correlation coefficient of mass flux and stagnation temperature fluctuations, $[(\rho u)'T_t'] / [\langle (\rho u)' \rangle \langle T_t' \rangle]$
$R_{T_t'v'}$	= correlation coefficient of stagnation temperature and vertical velocity fluctuations, $[T_t'v'] / [\langle v' \rangle \langle T_t' \rangle]$
Re	= Reynolds number
T	= temperature
u	= axial velocity
v	= vertical velocity
w	= lateral velocity
y	= distance normal to model surface
γ	= intermittency factor
δ	= boundary-layer thickness
ρ	= density
$\langle () \rangle$	= root mean square

Superscripts

$()'$	= fluctuating value
$()$	= time averaged

Subscripts

e	= boundary-layer edge
t	= total or stagnation conditions
θ	= momentum thickness

Introduction

WITH recent advances in numerical methods for computing compressible turbulent boundary layers, the need for developing accurate models and verifying existing models of the Reynolds shear-stress and turbulent heat-flux terms which appear in the conservation equations has become evident. This need resulted in increased efforts to measure these terms directly with hot-wire anemometers. The experimental uncertainties in hot-wire measurements in compressible flow are reflected in the limited amount of shear-stress data that have been reported.¹ While compressible subsonic² and supersonic³ turbulent shear-stress data obtained with hot wires gave reasonable agreement with shear-stress values obtained by integrating the conservation equations using measurements of the mean velocity and temperature profiles together with wall shear, the only reported data in hypersonic flow⁴ fell an order of magnitude below their expected values. Near the wall, all reported data²⁻⁴ show a systematic unexplained deviation from their expected values.

The problems of measuring Reynolds shear stress with a hot wire at hypersonic speeds are two-fold. First, it is necessary to obtain accurate measurements of the cross-correlations $(\rho u)'v'$ and $T_t'v'$. Previous techniques,^{3,4} based on a mode-diagram approach, determine these correlations indirectly and accurate measurements are difficult to obtain. For example, preliminary attempts to measure these correlations in the present flow with cross-wire probes failed because of problems associated with wire strain gauging and vibration. Such problems are most severe at hypersonic speeds, where very high temperatures are required to obtain an output that is sensitive only to mass flow fluctuations. Second, additional assumptions regarding the fluctuating flowfield are required to deduce the Reynolds shear stress $\bar{\rho} u'v'$ from these cross-correlations.

The present paper describes an alternate technique that was developed for the direct measurement of the cross-correlations, a technique which does not depend on the mode-diagram approach. Also developed were hot-wire probes that eliminate strain gauging and wire vibration completely. The measured cross-correlations were used to deduce the Reynolds shear stress and compared with shear stress distributions obtained from integration of the mean flow data in this equilibrium boundary layer. Furthermore, the direct measurements permitted, for the first time, an evaluation of the higher moments of the cross-correlations, thus giving in-

Received November 7, 1974; revision received May 19, 1975.

Index categories: Supersonic and Hypersonic Flow; Boundary Layers and Convective Heat Transfer-Turbulent.

*National Research Council Associate; now Scientist, Messerschmitt-Bölkow-Blohm, Munich, West Germany.

†Assistant Chief, Experimental Fluid Dynamics Branch. Associate Fellow AIAA.

sight into the statistical properties of shear stress at hypersonic speeds.

Description of Experiment

The investigation was conducted in the Ames 3.5 ft hypersonic wind tunnel. In this facility, high-pressure heated air flows through the 106.7-cm-dia test section to low-pressure spheres. The nominal freestream test conditions were: Mach number = 7.2, total pressure = 34 atm, and total temperature = 698 K. The test model was a cone-ogive cylinder, 330-cm long by 20.3 dia. Previous test results⁵ established the existence of a fully developed, self-similar turbulent boundary layer with a negligible pressure gradient from 100 to 300 cm from the model tip. The present measurements were obtained 175 cm from the model tip. The measured boundary-layer parameters at this station were approximately: edge Mach number = 6.85, boundary-layer thickness = 2.7 cm , Reynolds number based on boundary-layer thickness = 0.2×10^6 . The model wall temperature was 310 K. This flowfield is the same as reported in Ref. 6 where mass flow and stagnation temperature fluctuation measurements were obtained with conventional hot-wire probes using both constant current and constant temperature anemometers with mode diagram techniques, and in Ref. 5 where mean flow profiles of velocity and temperature at various locations along the surface are used to evaluate shear-stress and heat-flux profiles across this boundary layer.

Description of Probe Designs

The turbulent fluctuations were measured with specially designed probes using two basic configurations: One was a dual wire probe, for obtaining $(\rho u)'v'$, $(\rho u)'w'$, $\langle v' \rangle$, and $\langle w' \rangle$; and the other was a triple wire probe for determining

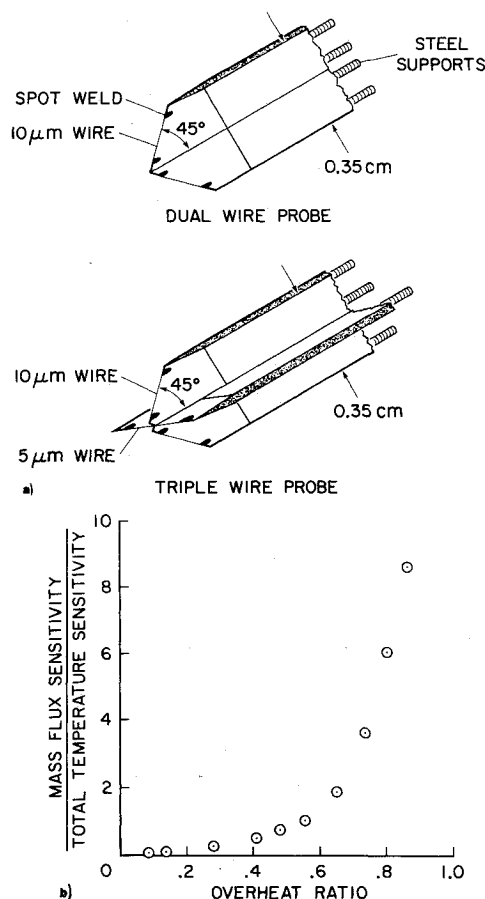


Fig. 1 a) Hot-wire probes; b) variation of sensitivity ratio with overheat ratio

$\overline{T_t'v'}$. The dual wire probe consisted of two 10-μm-diam platinum-rhodium wires mounted on a ceramic wedge as shown in Fig. 1a. The wires were first spot-welded onto steel supports, and then the open space between the wires and supports was filled with a high-temperature alumina-based ceramic paste to obtain complete fusion between the wires and the ceramic wedge. The ceramic was carefully removed from the front of the wire, exposing it to the flow. Care was taken to ensure that the wires were inclined exactly 45° to the probe axis.

Because of the heat loss into the substrate, constant temperature anemometers were used for operating the new probes. (Constant current anemometers can only be used for probes with well defined time constants.) Based on the conclusions of Ref. 6 this virtually eliminated the mode diagram technique since the constant temperature anemometer has little response to stagnation temperature fluctuations at low overheats. In addition, it has been shown⁷ that the transfer function of the constant temperature anemometer is a function of the overheat ratio and is particularly pronounced for thin film probes or wires supported by substrates. However, at high overheat ratios the transfer function is flat and virtually insensitive to overheat ratio.⁷ To obtain accurate turbulence measurements the present probes were operated at overheat ratios near 1.0. Previous measurements with single platinum-rhodium wires for the present flow conditions have shown for overheat ratios of 0.75 or higher the wires are predominantly mass-flux sensitive.⁶ This is illustrated in Fig. 1b where a typical variation of the ratio of mass-flux to total temperature sensitivity vs overheat ratio from Ref. 6 is shown for a platinum-rhodium wire at $y/\delta = 0.23$. Since the new probes used the same diameter wires they were also assumed to be responding to mass-flux and vertical velocity fluctuations only at overheat ratios above 1.0. This assumption was verified by additional measurements to be discussed later. The wire operating temperatures were as high as the oxidation temperature (1600K) with no apparent damage to the wire-ceramic bond.

The upper-frequency limit (−3 db) of the probes, as determined by the conventional square-wave technique, was approximately 100 kHz. One probe was also constructed with a thinner wire whose upper frequency limit was near 150 kHz. No difference could be observed in the measured fluctuation intensities with the two probes. Previous measurements⁶ for this flow (using constant current anemometers with 500 kHz response) have shown that 90% of the turbulent energy is contained within frequencies of 0–30 kHz.

The same design technique was employed to construct a triple wire probe by adding a second ceramic wedge at right angles to the dual wedge probe and putting a 5-μm diam platinum-rhodium wire on its tip, Fig. 1a. This third wire was operated near its recovery temperature with a constant-current anemometer. The smaller 5-μm wire was required so that adequate signal-to-noise ratios (20 to 1) could be achieved with the constant-current anemometer. When cross-correlating the ac signals from the different anemometers, all energy above 30 kHz was filtered out, since the frequency response characteristics of the two systems are different at high frequencies.

Due to the complicated steady-state heat conduction between the wires of the probes and the ceramic substrate, it was not possible to deduce the sensitivity of the wires from the slope of the steady-state calibration curve. The probes were calibrated by comparing their rms-outputs to the previously measured mass-flux intensities⁶ obtained with conventional hot wires across the boundary layer and in the local freestream. This method has the advantage of eliminating low-frequency problems common to dual film probes. For the present flow only a small percentage (less than 1) of the total turbulent energy is contained in this low-frequency interval where thermal feedback problems are important. For wires at yaw angles of 45° to the mean flow the sensitivity to vertical

velocity is exactly equal to the sensitivity to mass-flux. To minimize frequency and phase differences between the wires only those probes which gave similar responses to square wave tests using identical anemometers with identical gain and filter settings were used.

The obvious advantages of the new probes compared to conventional hot wires are their mechanical strength, the fixed geometry at all overheat ratios which permits the use of cosine-law cooling relationships, and the elimination of strain gauging and vibration signals. The present probes indicated "clean" spectra to 150 kHz.

Equations for Turbulent Shear Stress

The fluctuating quantities determined from hot-wire measurements in compressible turbulent flows are:

$$(\rho u)', v', w', T_t'$$

$$(\rho u)'v', (\rho u)'w', (\rho u)'T_t', T_t'v'$$

The cross-correlations can be expanded as follows:

$$(\rho u)'v' = \bar{\rho} \bar{u}'v' + \bar{u}\bar{\rho}'v' + \text{"higher-order correlations"} \quad (1)$$

$$T_t'v' = \bar{T}_t'v' + \bar{u}/C_p \bar{u}'v' + \text{"higher-order correlations"} \quad (2)$$

To obtain the Reynolds shear stress $\bar{\rho} \bar{u}'v'$ from hot-wire measurements alone, an assumption must be made concerning the term $\bar{u}\bar{\rho}'v'$ which, for high-speed compressible flows, has a magnitude greater than that of the shear-stress term. (Previous investigators³ and ⁴ have assumed the correlation between pressure and velocity fluctuations to be negligible.) Then, expanding the equation of state, multiplying by v' and time averaging, we obtain a relation between density and temperature correlations with velocity:

$$\bar{\rho}'v' = 0 = R(\bar{T}'v' + \bar{\rho}\bar{T}'v') \quad (3)$$

If we combine Eqs. (1-3), the equation for obtaining Reynolds shear stress becomes,

$$\bar{\rho} \bar{u}'v' = [C_p \bar{T}'v' / C_p \bar{T}' + \bar{u}^2] [(\rho u)'v' + \bar{u}\bar{\rho}'v' / \bar{T}'v'] \quad (4)$$

Since the pressure fluctuations increase with Mach number, this assumption of zero correlation between pressure and velocity fluctuations becomes questionable for hypersonic flows. Equation (4) was used to deduce the Reynolds shear stress from the present measurements; the results are discussed in the following section. The turbulent heat flux $(T_t'v')$ was measured directly with the triple probe.

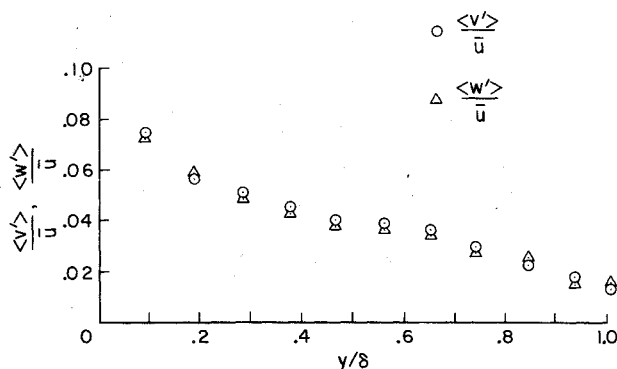


Fig. 2 Vertical and lateral velocity fluctuation distribution across the boundary layer.

Discussion of Results

Turbulence Intensities

Figure 2 shows the measurements of the rms vertical velocity ($\langle v' \rangle$) and lateral velocity ($\langle w' \rangle$) through the boundary layer. The data were obtained from the instantaneous difference of the dual probe signals by rotating the probe 90° on two successive runs. The two fluctuating velocity components are of equal magnitude throughout the boundary layer, contrary to incompressible boundary layers, where $\langle w' \rangle$ is generally larger than $\langle v' \rangle$.

Mass-Flux-Total-Temperature Cross-Correlation

To test the accuracy of the new probes, a direct comparison of the mass-flux total-temperature correlation coefficient measured by a single normal wire using the mode diagram technique⁶ and the triple wire probe was made. For the triple wire probe, the correlation coefficient was measured directly by correlating the ac signal from the 5- μ m temperature wire with the instantaneous sum of the ac signals from the two 45° wires. The comparison is shown in Fig. 3. The reasonable agreement between the two sets of data across the entire boundary layer gives added assurance that the two 45° wires at high overheats are responding to mass-flux fluctuations only and the third normal wire at low overheat to total temperature fluctuations only.

Turbulent Heat Flux

The total turbulent heat-flux correlation coefficient was obtained using the triple wire probe. The time-varying signal from the normal wire, operating at low overheat (corresponding to total temperature fluctuations), was cross-correlated with the time-varying signal that represented the instantaneous difference of the two 45° wires, operating at high

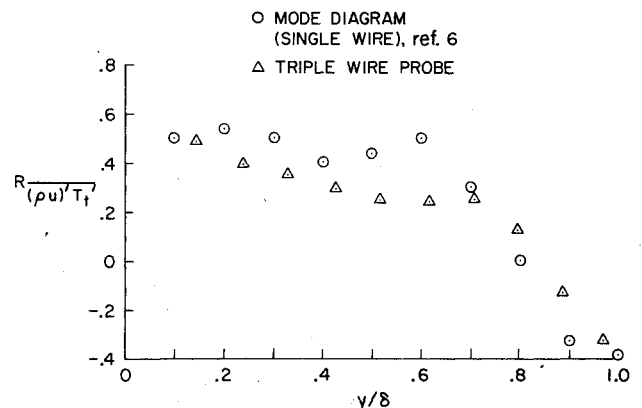


Fig. 3 Mass-flux stagnation temperature cross-correlation coefficient distribution across the boundary layer.

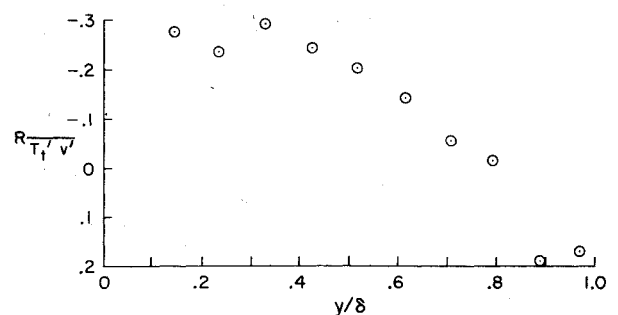


Fig. 4 Vertical velocity stagnation-temperature cross-correlation coefficient distribution across the boundary layer.

overheat (corresponding to vertical velocity fluctuations). The measured values of the cross-correlation coefficient are presented in Fig. 4. Using measured values of $\langle v' \rangle$ (Fig. 2) and $\langle T_t' \rangle$ (Fig. 4 from Ref. 6), we evaluated the total turbulent heat flux $\overline{T_t' v'}$. The resultant values are compared in Fig. 5 with the turbulent heat flux obtained by integrating the energy equation, using measured profiles of mean-velocity and temperature. The agreement of the present data with the mean-flow integration values is reasonably good in the outer half of the boundary layer, but the present values are lower near the wall. Since the overall probe diameter was approximately 13% of the boundary-layer thickness, interference effects between the probe and the wall are possible causes for these differences. In addition, uncertainties in the wire calibration and the stagnation temperature fluctuation data from Ref. 6 could cause these differences. Wire length effects should not be important since most of the turbulence energy is contained in scales significantly larger than the wire lengths used. Considering all sources of errors the disagreement between the measured and mean-flow integration values are not unreasonable.

Turbulent Reynolds Stresses

The cross-correlation coefficients $R_{(\rho u)'v'}$ and $R_{(\rho u)'w'}$ were evaluated by correlating the instantaneous sum and difference of the signals from the two 45° wires of the dual wire probe. The two coefficients were obtained during two consecutive test runs during which the boundary layer was traversed using the same probe, but rotated 90° for the second traverse. Figure 6 shows variations of the two correlation coefficients across the boundary layer and Fig. 7 shows the corresponding normalized values of $(\rho u)'v'$ and $(\rho u)'w'$. The lateral cross-correlation coefficient is consistently lower than the vertical one, except beyond $y/\delta=0.8$, where it becomes higher.

The magnitude of the lateral cross-correlation $(\rho u)'w'$ is surprising. While the present lateral cross-correlation data are of the same order as the vertical cross-correlation data,

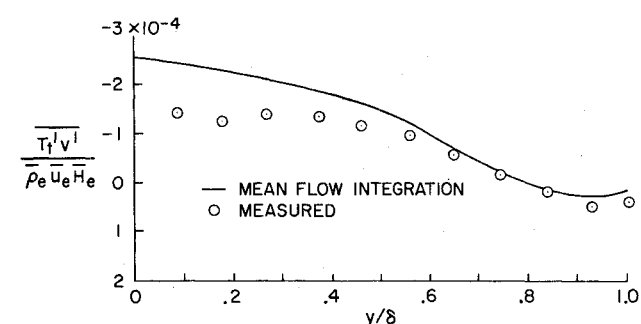


Fig. 5 Turbulent total heat-flux distribution across the boundary layer.

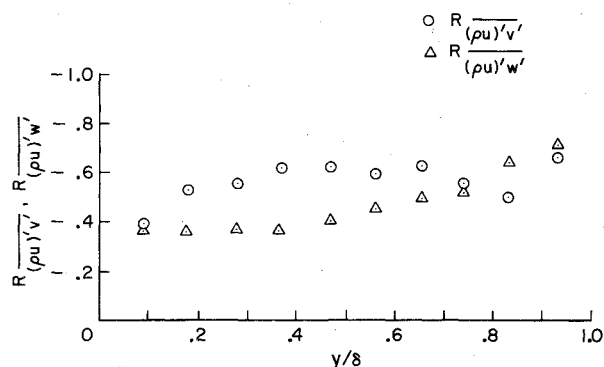


Fig. 6 Mass-flux vertical and lateral cross-correlation coefficient distribution across the boundary layer.

previous incompressible⁸ and subsonic compressible² measurements in two-dimensional, and axisymmetric flows have shown that the lateral cross-correlation is negligible compared to the vertical cross-correlation. The significance of the present measurement is not fully understood at present. To ensure that three-dimensional flow effects were not present for these tests, detailed surface skin-friction and mean flow-field measurements were obtained at 90° intervals around the model.² Variations in the data around the model were within the experimental accuracy of the measurements. In addition, several tests were made with the dual hot-wire-probe axis misaligned with the model axis up to 5° in both directions at 180° intervals around the model. The resulting lateral cross-correlations were in close agreement with the results shown in Fig. 7. Therefore, it is believed that the three-dimensional flow effects are not influencing the present measurements. Tests were also performed to ensure that instrumentation and probe errors were not present. Although preliminary measurements obtained with conventional cross-wires using constant current anemometers gave inconsistent results, all the lateral cross-correlation measurements obtained in the present flow indicated nonzero values. These results were obtained using both the mode-diagram and the direct-measurement techniques. Finally, as a check on the present instrumentation and data reduction techniques, similar measurements were obtained in a subsonic channel flow. As opposed to the present high-Mach number data, the subsonic results indicated that the lateral cross-correlations were negligible compared to the vertical cross-correlations.

The shear stress was evaluated using Eq. (4), which requires the assumption discussed previously. The resulting shear stress values are compared in Fig. 8 with those obtained by integrating the momentum equation using measured profiles of mean velocity and mean temperature. It should be noted that measured values of $T_t' v'$ were used in evaluating Eq. (4) and that the measured values were somewhat lower than results from the mean flow integration. However, even when the mean-flow integration values for $T_t' v'$ were used in Eq. (4), the resulting shear stress increased only slightly, as indicated

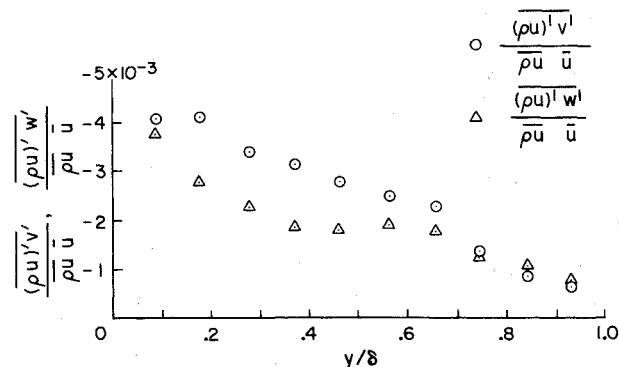


Fig. 7 Normalized mass-flux vertical and lateral cross-correlation distribution across the boundary layer.

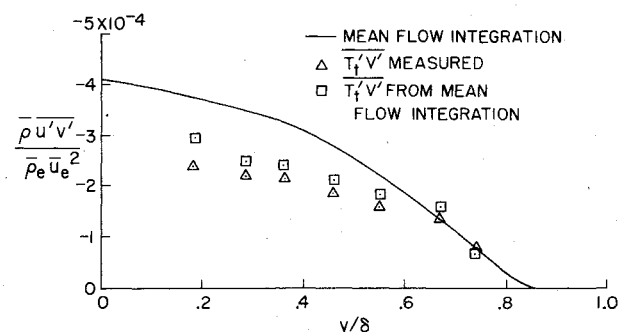


Fig. 8 Reynolds shear-stress distribution across the boundary layer.

in Fig. 8. In the inner half of the boundary layer, the data are consistently lower than the mean-flow integration values. In addition to the possible errors mentioned previously, the assumption of a zero-pressure vertical velocity correlation is another possible error source. In view of these uncertainties the disagreement between the data and mean-flow integration values is not significant.

Statistical Properties of the Turbulent Fluctuations

High moments of the turbulent fluctuations and their cross-correlations were also determined and compared with previous incompressible measurements⁸ and ⁹ to test the statistical similarity of compressible and incompressible boundary layers. Figures 9 and 10 show the dimensionless third (skewness) and fourth (flatness) moments of the mass flux and vertical and lateral velocity fluctuations. The intermittency distributions shown in Fig. 11 were calculated using the flatness factor data. It is seen that the vertical and lateral velocity components have statistical properties similar to the mass flux fluctuations. The present data and those

taken from Ref. 6, which were obtained using a single wire probe, compare very well. Because of their size, the wedge probes used in the present investigation could not detect the wall intermittency for $y/\delta < 0.1$. At the outer edge, the skewness and flatness factors tend to increase, indicating a non-Gaussian probability distribution with intermittency. Significant differences between the intermittency results (Fig. 11) and the data of Klebanoff⁸ are apparent at the outer edge of the boundary layer.

Figures 12-14 show the skewness, flatness, and intermittency factors of the cross-correlations. Their distribution across the boundary layer are markedly different from any of their individual components. The skewness of $(\rho u)'v'$ and $(\rho u)'w'$ is negative across the entire boundary layer, and flatness factors of these cross-correlations are greater than three. They are very nearly equal in their statistical behavior, except in the wall region where $(\rho u)'w'$ has larger skewness and flatness than $(\rho u)'v'$. This could be due to the sensor positions, which are not affected as much by turbulence gradients for the $(\rho u)'w'$ measurement as it is for the $(\rho u)'v'$ measurement. The flatness factors and intermittency are largest in the wall region for both correlations,

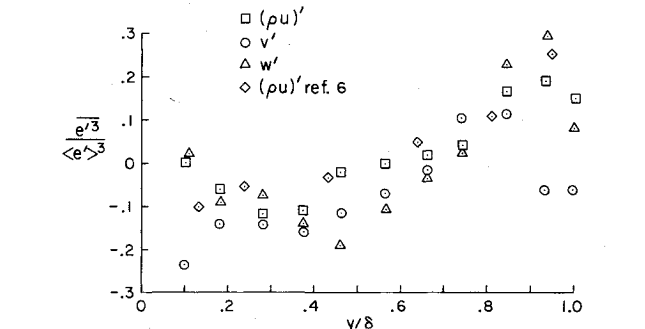


Fig. 9 Third-moment (skewness) distribution of the mass flux and vertical and lateral velocity fluctuations across the boundary layer.

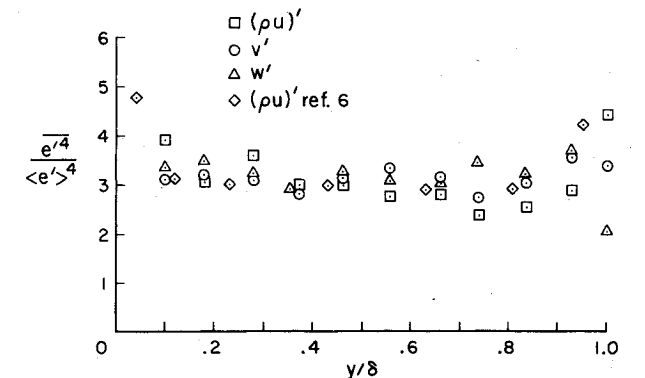


Fig. 10 Fourth-moment (flatness) distribution of the mass flux and vertical and lateral velocity fluctuations across the boundary layer.

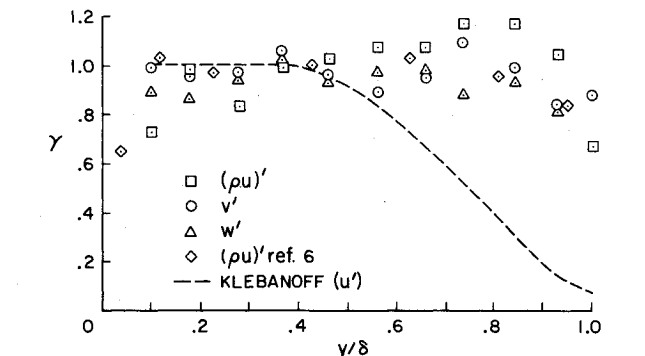


Fig. 11 Intermittency distribution of the mass flux and vertical and lateral velocity fluctuations across the boundary layer.

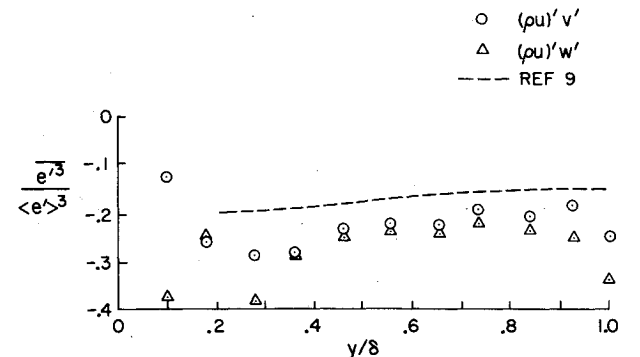


Fig. 12 Third-moment (skewness) distribution of the mass-flux vertical and lateral velocity cross-correlations across the boundary layer.

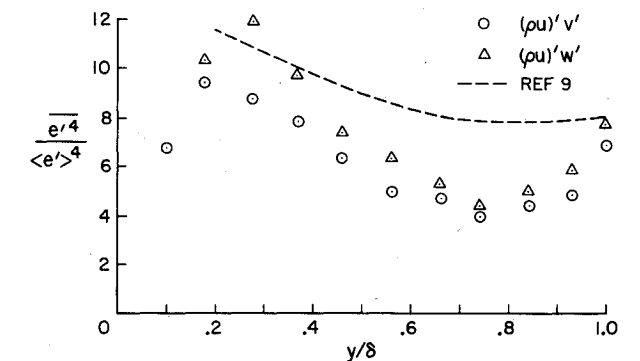


Fig. 13 Fourth-moment (flatness) distribution of the mass-flux vertical and lateral velocity cross-correlations across the boundary layer.

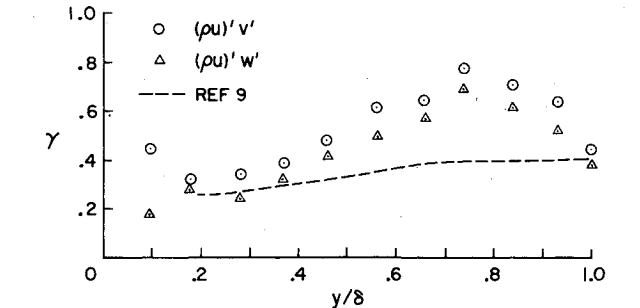


Fig. 14 Intermittency distribution of the mass-flux vertical and lateral velocity cross-correlations across the boundary layer.

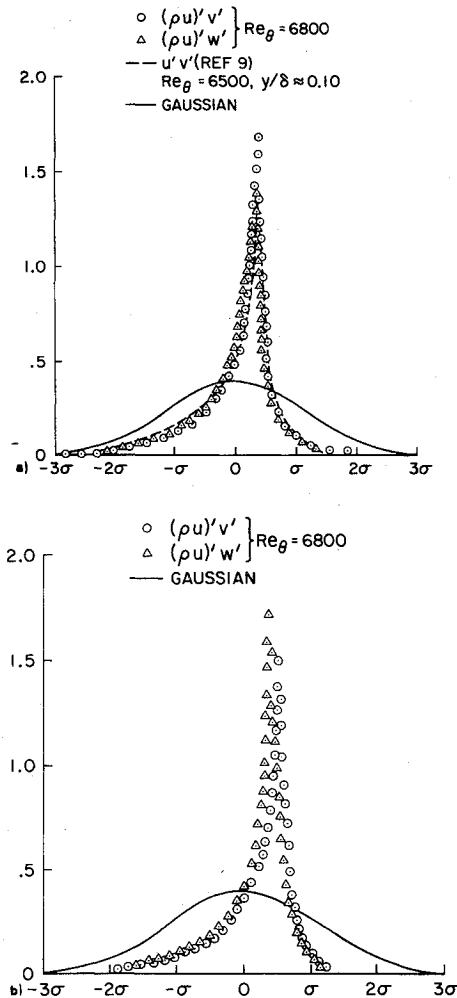


Fig. 15 Probability density distributions of the mass-flux vertical and lateral velocity cross-correlations: a) $y/\delta = 0.18$; b) $y/\delta = 0.66$.

indicating that the turbulent shear stress is produced mainly near the wall in a hypersonic boundary layer, as is the case for incompressible boundary layers.

In Figs. 12-14, these results are compared with incompressible measurements⁹ of the higher moments of $(u'v)$ obtained with a standard crossed-wire probe in a flow with a momentum thickness Reynolds number of 6500. The present hypersonic data were obtained at a Reynolds number based on a momentum thickness of 6800. The comparison shows that the statistical behavior for the two flows are similar. Both flows have turbulent stresses that are negatively skewed and highly intermittent through the entire boundary layer, in contrast to their individual components.

The statistical similarity between the cross-correlations $(u'v')$, $(\rho u)'v'$, and $(\rho u)'w'$ is also apparent in their probability density distributions, which are shown for two positions in the boundary layer in Fig. 15. The non-Gaussian distribution reflects their strong skewness.

Figure 16 shows, for two locations in the boundary layer, the normalized power spectra of the mass-flux, vertical and lateral velocity fluctuations as well as of the mass-flux vertical and lateral velocity cross-correlations. The power spectra for the fluctuations were obtained from Fourier transforms of their auto-correlation functions, and the spectra for the cross-correlations were obtained from Fourier transforms of the cross-correlation functions. The turbulent intensities and their cross-correlations have nearly the same power spectra. Previous incompressible measurements¹⁰ have shown that the quantities $\overline{u'^2}$, $\overline{v'^2}$, and $\overline{u'v'}$ also have the same power spectra.

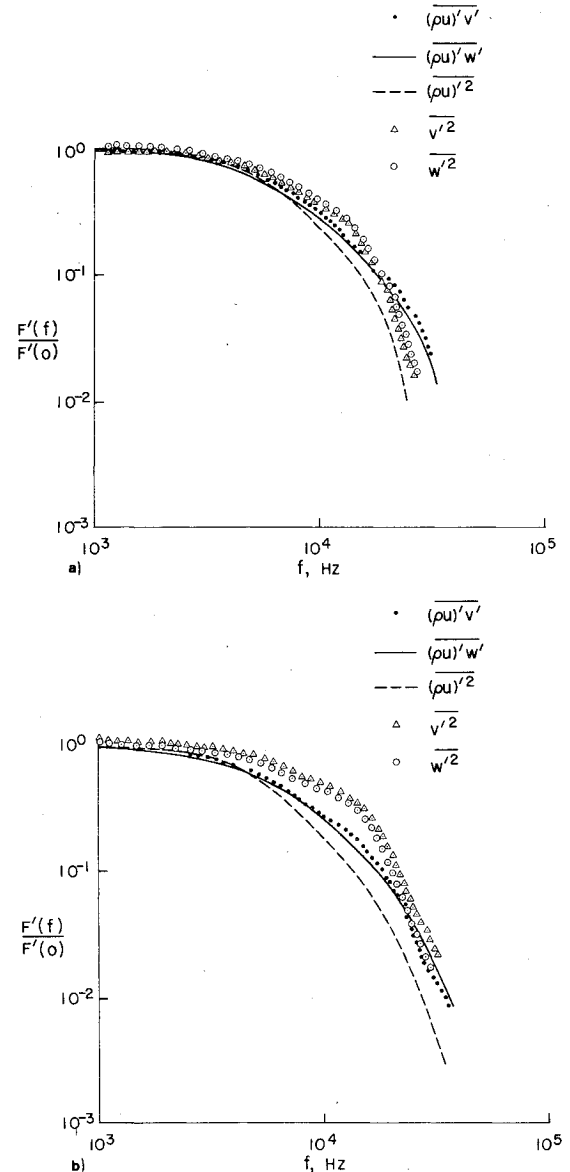


Fig. 16 Normalized power spectra of the fluctuating quantities and their cross-correlations: a) $y/\delta = 0.18$; b) $y/\delta = 0.66$.

Conclusions

The present paper describes two new hot-wire probes used for turbulence measurements in a compressible flow. It is demonstrated that the probes can directly measure cross-correlation coefficients in heated hypersonic flows. Unlike standard crossed-wire probes, the new probes can be operated at extreme overheat ratios without the usual strain-gauging, wire-slack, and oscillation problems.

For the first time, a direct measurement of total heat flux in a turbulent nonadiabatic hypersonic boundary layer was made. The measurement agrees reasonably well with values of the heat flux obtained by integrating the energy equation using measured velocity and temperature profiles. The turbulent shear stress measurement based on this total heat flux measurement, the mass-flux vertical-velocity cross correlation measurement, and the zero-pressure vertical-velocity correlation assumption is also in reasonable agreement with values obtained by integrating the momentum equation. This agreement is in sharp contrast to previous hypersonic results.⁴

The statistical properties of the two cross-correlations $(\rho u)'v'$ and $(\rho u)'w'$, presented in terms of skewness, flatness, intermittency, and probability density distribution,

show a striking similarity to statistical properties of the incompressible instantaneously Reynolds shear stress.

References

- ¹Sandborn, V. A., "A Review of Turbulence Measurements in Compressible Flow," NASA, TM X-62,337, March 1974.
- ²Gibbings, J. C. and Mikulla, V., "Measurements of Reynolds Stresses in Compressible Flow," Aeronautical Research Council Rept. 34540 FM4408, 1973, London, England.
- ³Rose, W. C. and Johnson, D. A., "A Study of Shock Wave Turbulent Boundary Layer Interaction Using Laser Velocimeter and Hot-Wire Anemometer Techniques," AIAA Paper 74-95, Washington, D.C., 1974.
- ⁴Demetriades, A. and Laderman, A. J., "Reynolds Stress Measurements in a Hypersonic Boundary Layer," *AIAA Journal*, Vol. 11, Nov. 1973, p. 1594.
- ⁵Horstman, C. C. and Owen, F. K., "Turbulent Properties of a Compressible Boundary Layer," *AIAA Journal*, Vol. 10, Nov. 1972, pp. 1418-1424.
- ⁶Owen, F. K. and Horstman, C. C., "Turbulent Measurements in an Equilibrium Hypersonic Boundary Layer," AIAA Paper 74-93, Washington, D.C., 1974.
- ⁷Mikulla, V., "The Measurements of Intensities and Stresses of Turbulence in Incompressible and Compressible Air Flow," Ph.D. Thesis, Aero. Eng. Dept., University of Liverpool, England, 1973.
- ⁸Klebanoff, P. S., "Characteristics of Turbulence in a Boundary Layer with Zero Pressure Gradient," NACA Rept. 1247, 1955.
- ⁹Gupta, A. K. and Kaplan, R. E., "Statistical Characteristics of Reynolds Stress in a Turbulent Boundary Layer," *Physics of Fluids*, Vol. 15, June 1972, pp. 981-985.
- ¹⁰Sandborn, V. A. and Brown, W. H., "Turbulent Shear Spectra and Local Isotropy in the Low-Speed Boundary Layer," NACA TN 3761, Sept. 1956.

From the AIAA Progress in Astronautics and Aeronautics Series . . .

HEAT TRANSFER AND SPACECRAFT THERMAL CONTROL—v. 24

Edited by John W. Lucas, Jet Propulsion Laboratory

This volume presents a review of the state-of-the-art of thermophysics in aerospace, surface radiation properties, thermal joint conductance, heat transfer, multilayer insulation, and thermal control devices.

A critical review of aerospace thermophysics examines the tasks presented by the space shuttle and space stations, including thermal control surfaces having lifetimes up to 20 years. Other studies examine degradation and stabilization of thermal control coatings, with radiant heat transfer calculations. The emittance of several coated and uncoated metal surfaces is calculated, with data on time and exposure degradation.

Thermal joint conductance studies examine prediction of conductance, heating rates, and the influence of interstitial fillers on heat transfer. Other papers cover heat transfer modeling, transient heat flow in structures, and the special heat transfer problems of multilayer insulations, both in structures and in space suits.

Papers dealing with thermal control devices discuss selection criteria, mutual interaction between electric and thermal conduction, and thermal efficiency of various materials used in spacecraft structures.

658 pp., 6 x 9, illus. \$14.00 Mem. \$20.00 List

TO ORDER WRITE: Publications Dept., AIAA, 1290 Avenue of the Americas, New York, N. Y. 10019